IJAAR PUBLISHING®

Engineering Research Journal | ISSN: 2782-8212
Vol. 5, Issue 2 (2025) | www.ijaar.org/erj

Design and Fabrication of Experimental Shell and Tube Heat Exchangers for Distilled Water Production

Sinebe, J.E.
Department of Mechanical Engineering, Delta State University, Abraka, Nigeria
jesinebe@delsu.edu.ng

Abstract: *This study was conducted to design, analysis, and fabricate a tube heat exchanger prototype for producing distilled water. The Apparatus has three main system components: the shell side, tube side, and baffles. The shell and tube sides are made of galvanised steel, and the baffles are arranged in segments. A pressure gauge measures the amount of pressure in any section of a pipe. The test was carried out using a heater with a capacity of six litres, or approximately 0.006 m^3. The heater, pumps, and tanks were all connected by pipes, having 21.34 mm diameter, and 12.70 mm long. The results revealed that at extremely high temperatures above atmospheric conditions, the water transforms into steam, which is then converted back to water through heat exchange. When considering the shell and tube sides of a heat exchanger, the temperature curve agrees very well with experimental data.*

Keywords: Distilled water, heat exchanger, model, shell and tube, water potability

Sinebe, J.E. (2025). Design and Fabrication of Experimental Shell and Tube Heat Exchangers for Distilled Water Production. *Engineering Research Journal. 5*(2), 10-21. DOI: 10.5281/zenodo.15192079

1.0 Introduction

The demand for water potability and heat exchangers in the domestic and industrial sectors is increasing globally; hence, there is paramount necessity for the design and development of more effective heat exchangers. A shell and tube heat exchanger (STHE) is a popular apparatus widely utilized in numerous engineering applications, mainly in the oil and gas, mechanical, food processing and chemical sectors. This is primarily attributed to its simplicity in design, operation, and elevated pressure drop ability. Increasing economic benefits, and lowering the shell and tube costhave become major menace in industrial applications. Most traditional heat-exchanger design approaches, such as plain tube and normal segmental baffle, have been produced already for STHE sizing (Yang et al., 2020; Chen et al., 2022). Various algorithms and optimisation approaches are used in these methods, including SA (simulated annealing) (Rao et al., 2017; Estupiñán-Campos et al., 2024), MINLP (mixed integer nonlinear programming) (Lee & Leyffer, 2011), tube count table algorithm (Math, 2021; Ghasem, 2021), GA (genetic algorithms) (Ponce-Ortega et al., 2009), and MILP (mixed integer linear programming) (Gonçsalves et al., 2016). Nonetheless, a comparativelygreat exchanger region, within high heat duties tends to result from poor utilization effectiveness of the exchanger geometries, which is basically followed by high economic and labor costs involvement.To overcome these bottlenecks, advanced heat transfer enhancement (HTE) methods, are typically being formulated to enhance STHE functionality, through adequate alteringof their surface or structure. The primary benefits of heat transfer enhancement applications in various fields include: reduction in the required exchanger area for STHE design; evading additionof extra space, and connectingother exchangers for retrofit purposes; and enhancing the transformation of pressure drop to heat transfer coefficients, to prevent surpassing the system's capacity (Bhattacharyya *et al.*, 2022; Mukhlif & Abed, 2024).

Heat Transfer Enhancement approaches, may be primary characterized into tube-side enrichment (TSE) and shell-sideenrichment(SSE) categories. TSEcategory (technique) can be further sub-divided into: tube inserts (coiled-wire, twisted-tape) and internal fins, which have the potential of creating an increment in the heat transfer functionality, and the STHE geometrical zone. Remarkably, helical baffles and external fins are employed as the SSE intensified systems. In comparison with the segmental barriers, the conversion degree from the pressure drop to heat transfer rate tends to be inclinedconsiderably, by utilizing the helical screens. Notably, the external fins are equivalent to internal fins; hence, they have the ability of lengthening the surface area by 200 – 400%. Additionally, relevant and reliable techniques have been scientifically produced by numerous researchers (Hamza et al.., 2022; Fernandes, 2023; Rahman, 2024). Recently, anthropogenic actions have led to various design qualities, than employing existing STHEdesigns. This can be attributed to the different unit operations to converge the software, which include: selection of baffle brand and tube insert, regulation of the tube pitch, tube dimensions and twisted pitch. These activities can lead to fluctuating degrees of nonconformity for various users; thereby, increasing the computation duration (Yang et al., 2020; Han et al., 2025).

Interestingly, to address the prevailingchallenges, this study aims to expand the documented STHE models, to obtain an efficient and computerized heat exchanger, through heat transfer improvement. The GDP was used in this work (model) to identify and indicate all the discrete decisions, most notably the tube passes quantity, TEMA tube scopes, helical angle, and tube arrangements. Tandiroglu *et al.* (2007) examined the effects of flow geometry attributes on transitory forced convective heat transfer, mainly for turbulent flow with round tube environment with baffles, to investigate variations in Nusselt number. The experiment

focused on variations in baffle spacing and angles, where 9 stainless steel partitions were installed, and the Re ranged from 3000 to 200000.It was noted that tubes with barriersincorporated performed better, when compared to the smooth tubes. Nu values increased in tubes with screens. Each researcher tried immensely to reduce the volume of heat losses, and these researches have been documented (Milani *et al.*, 2018; Mohammadi *et al*., 2020; Jayranaiwachira *et al.*, 2023) to configure a STHE. They adopted a pattern where the heat transfer coefficient was greatly upgradedupon, by installing appropriate sealers on the shell side. STHE are among the most commonly used thermal apparatus in the industries, this is because it offers great heat exchange area, within a smaller volume. Remarkably, these authors built there system from a different materials, which have ability to withstand varieties of fluids.

Kern and Bell-Delaware methods are the most commonly used strategies for designing STHE. The Kern techniquecontemplatesa single stream that flows in wavy pattern via heat exchanger shell. Likewise, the Bell-Delaware approach uses five parameters,to amend the shell-side heat transfer coefficient (h). This provides more preciseforecasting for the actual thermal and hydraulic performance, in shell-side and pressure drop calculations by accounting for leakage and bypass effects.Numerous studies on STHE optimisation use deterministic techniques (Ponce-Ortega et al., 2009; Ravagnani and Caballero, 2007) or metaheuristic algorithms (Patel and Rao, 2010). The mathematical model's nonlinearity, lack of convexity, and presence of continuous and discrete variables make STHE optimisation difficult. Typically, a single tool is used to optimise STHE; however, having several optimisation strategies in a toolbox may be useful for analysing the benefits and drawbacks of each.

2.0 Materials and Methods

2.1 Materials selection

Generally, the two materials used for the heat exchangers model construction were galvanized steel for the pipes, coated aluminum for the table platform, and aluminum for the heaters. These materials are known for their optimal thermal properties, and corrosion resistance, with the majority of the differences being application-specific.

2.2Design of Shell and Tube

2.2.1 Design of shell

Using TEMA STHE designation standards.

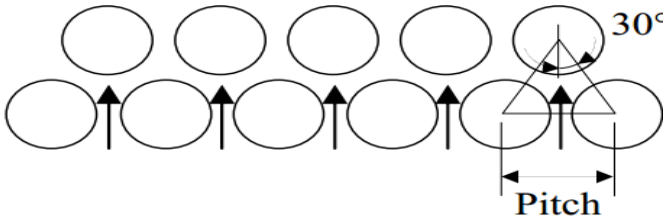
Shell Area (A_s) = $\frac{B \text{ x } C \text{ x } D_s}{P_t}$ 1

Mass Velocity (G_s) =$\frac{M_s}{A_s}$ 2

Reynolds number (R_e) = $\frac{G_s \text{ x } D_e}{\mu}$ 3

Where: A_s= shell area; B = baffles; C = clearance ($P_t - d_o$); D_e = equivalent shell diameter; m_s = fluid velocity on shell side; and P_t = tube pitch.

Since the tube pitch is arranged in a triangular manner (Triangular Pitch), it becomes necessary to obtain the effective diameter at the shell side (SS) to obtain the*h*in the shell side.



Triangular (30°)

Figure 1: Triangular pitch configuration of tube in the shell side

$$D_e = \frac{4 \text{ x } (\frac{\sqrt{3}}{4} p_t{}^2 - \pi \text{ x } d_o{}^2)}{\frac{\pi d_o}{2}} \quad 4$$

Where: $d_o = outer\ diameter.$

For SS heat transfer coefficient;

$$JH = \frac{h_o \text{ x } D_e}{K} \text{x } (\frac{C_u}{K})^{-0.33} \text{ x } (\frac{\mu}{\mu_w})^{-0.14} \quad 5$$

Where: h_o = from Reynolds graph between R_e and JH; K = thermal conductivity; μ_w = water dynamic viscosity; D_e = equivalent diameter of shell; C = SS specific heat; and μ = shell fluid dynamic viscosity at room temperature.

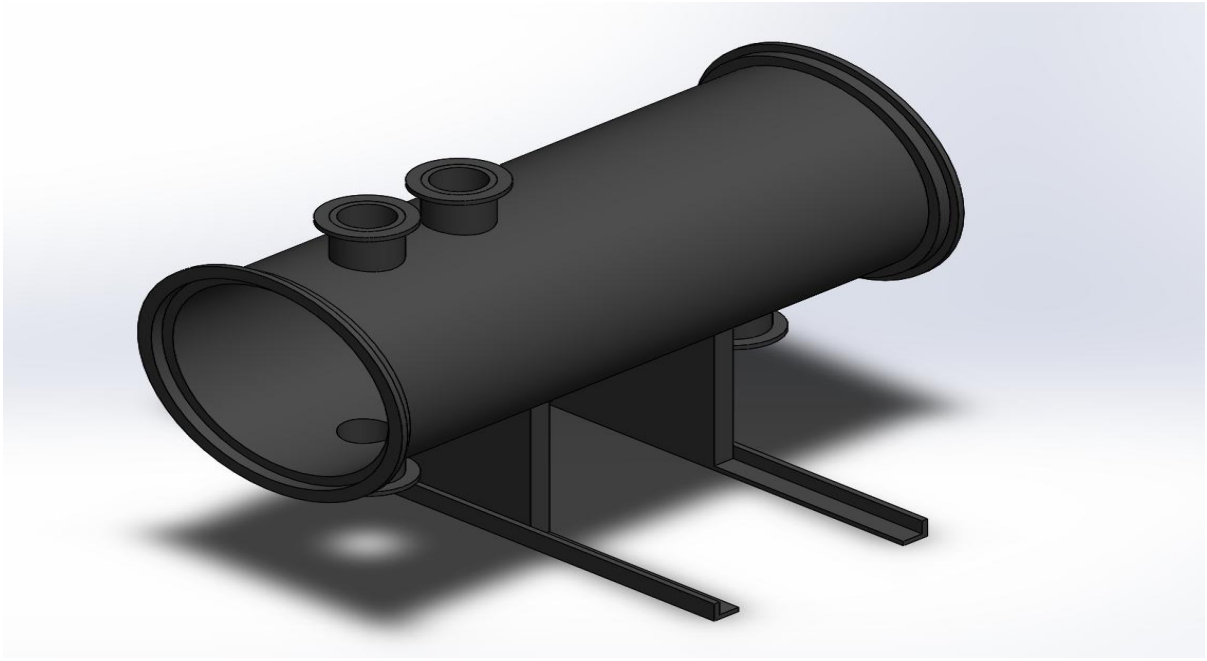


Figure 2: Design of the Shell made on solid works

2.2.2 Design of tube

$$A_t = \frac{\boldsymbol{A}' \text{ x } N_t}{Number\ \ of\ passes} \quad N_t = \frac{A}{\boldsymbol{A}'} \quad 6$$

Where: N_t = tubes numbers; A = total outside surface area of tubes; $A^{'}$ = outside surface area of one tube $A^{'} = \pi \text{ x } d_o \text{ x } l$.

$$G_t = \frac{M_t}{A_t} \quad 7$$

By obtaining the mass velocity we can now calculate Reynolds number;

$$R_e = \frac{G_t \text{ x } d_i}{\mu} \quad 8$$

For tube side heat transfer coefficient (h);

$$JH = \frac{h_i \text{ x } d_i}{K} \text{x } (\frac{C_u}{K})^{-0.33} \text{ x } (\frac{\mu}{\mu_w})^{-0.14} \quad 9$$

Where: h_i = from Reynolds graph between R_e and JH; K = thermal conductivit; μ_w = dynamic viscosity of steam; D_e = equivalent diameter of shell; d_i = inside diameter of tube size; C = specific heat of tube side fluid; and μ = tube fluid dynamic viscosity at room temperature.

$$h_{io} = \frac{h_i \text{x } d_i}{d_o} \quad 10$$

For the Tube outside heat h;

$$U_d(calc) = \frac{1}{h_{io}} + \frac{1}{h_o} + \frac{d_o}{d_i} + \frac{d_o \text{ x } \ln(\frac{d_o}{d_i})}{2k} + R_o \quad 11$$

Neglecting Fouling factor, tube outside h following checking the condition for accurate design ($\mathbf{0} < \frac{\boldsymbol{U_d(calc) - U_d(assumed)}}{\boldsymbol{U_d(assumed)}} < \mathbf{30\%}$).

This means that an accurate design yields a value less than 30% of the h. With the following parameters, the actual values from the formulas derived.

From the shell and tube design: number of tubes = 7; shell outer diameter = 250mm; shell inner diameter = 12.7mm; length of shell = 100mm; tube outside diameter = 12.7mm; tube inside diameter = 9.5mm; length of tube = 90mm; baffle spacing = 15mm (25%); tube pitch = 15.875mm; and number of passes = 2.

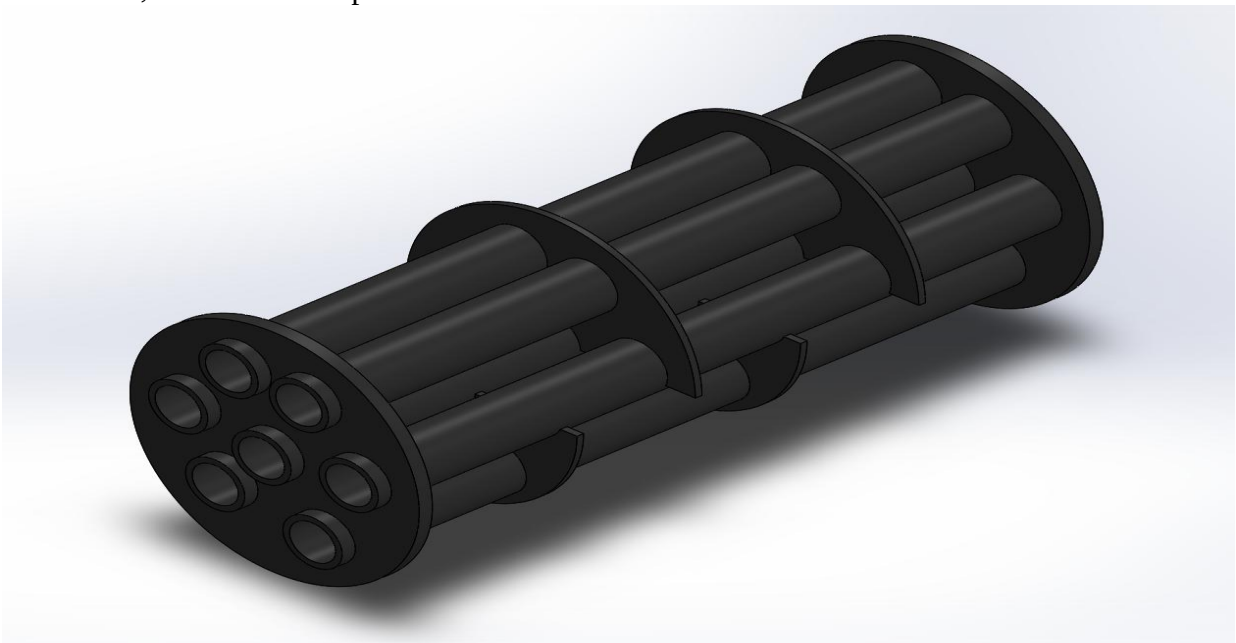


Figure 3: Design of the tubes made on solid works

2.2.3 Design of pipe cross section

Bernoulli's principle on flow system describes the relationship between pressure, velocity, and elevation. The application of this principle was considered;

$$P + \rho V^2/2 + \rho gh = CONST \quad 12$$

Where: P is the static pressure; $\frac{\rho V^2}{2}$ is the dynamic pressure; and ρgh is the hydrostatic pressure.

Comparing flow in pipes at 2 different locations, we use Bernoulli's;

$P_1 + \rho V_1^2/2 + \rho g h_1 = P_2 + \rho V_2^2/2 + \rho g h_2$ 13

When there is no change in elevation;

$P_1 + \rho V_1^2/2 = P_2 + \rho V_2^2/2$ 14

In static form;

$P_1 - P_2 = \rho/2\ (V_2^2/2 - V_1^2/2)$ 15

If the mass flow rate is equal;

$\dot{m}_1 = \dot{m}_2$ 16

$A_1 V_1 = A_2 V_2$ 17

This equation leads to continuity equation and conservation of mass

When $V_2 > V_1$, the velocity of the flow increases as it flows into the smaller diameter pipe.

$P_1 - P_2 = \rho V_1^2/2\ (A_1^2/A_1^2)$ 18

Since the velocity increases between point 1 and 2, the pressure must decrease. The sum of the static pressure and dynamic pressure equals stagnation pressure.

$P_2 = P_1 + \rho V_1^2/2$ 19

Venturimeter is used to measure fluid velocity or flow speed;

$Q = A_1 V_1$ 20

$V_1 = [2(P_1 - P_2)/\rho(A_1^2/A_1^2) - 1)\ ]^{1/2}$ 21

$Q = A_1 [2(P_1 - P_2)/\rho(A_1^2/A_1^2) - 1)\ ]^{1/2}$ 22

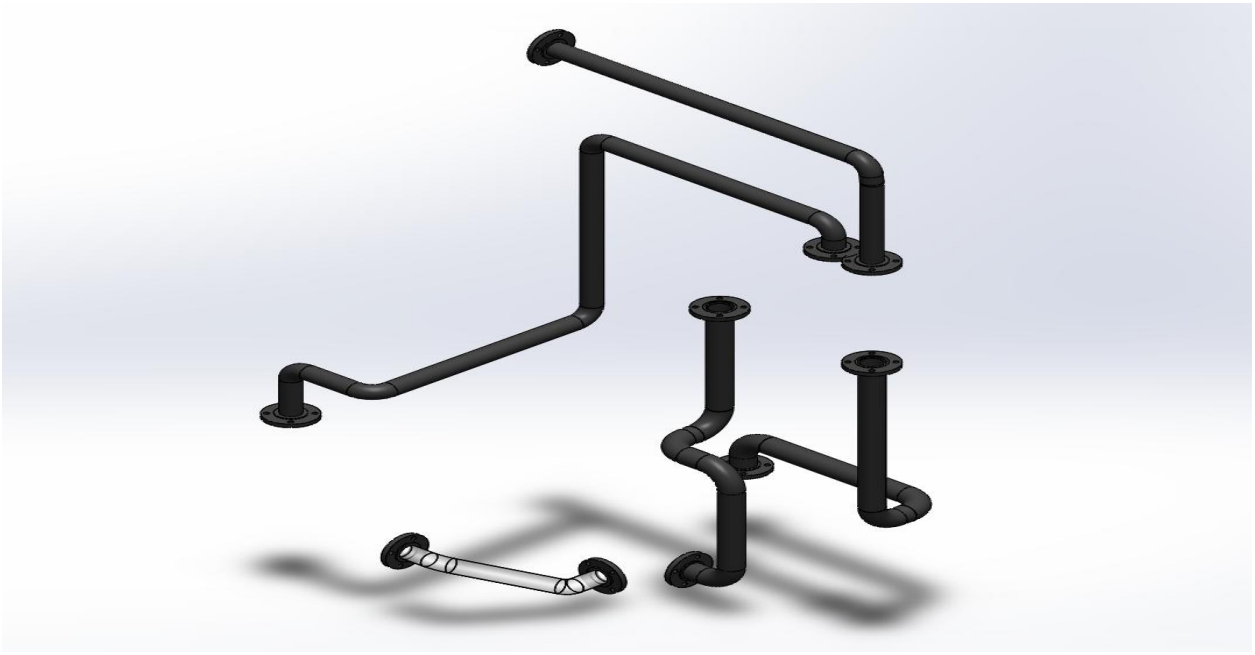


Figure 4: Pipe cross sectional diagram at different sections on solid works

2.2.4 Pump design

For Viscosity $(v) = \mu/\rho$ 23

Reynolds Number $(Re) = \rho VD/\mu$ 24

Where: $\mu =$ dynamic viscosity (mPa-s); $v =$ kinematic viscosity (mm^2/s); $\rho =$ density (kg/m^3); and $D =$ diameter of pipe (m).

At 100℃ (using viscosity tables): $v = 0.294\text{x } 10^{-6} m^2/s$; $\mu = 0.282 \text{ x } 10^3\ Ns/m^2 \rho = 1000\ kg/m^3$.

Since flow through the pipe is laminar;

Pump Input power, P (hp) = $\frac{\text{Q x H x } \rho}{75 \text{ x } \eta}$ 25

Where: Q = flow rate (m^2/s); H = total head developed in metres (m); ρ = density kg/m^3); and η = efficiency of Pump.

$\eta_o = \eta_p x \eta_m$

Where: pump rating = $0.5hp$ $(0.367\ kw)$ and pump discharge$(Q) = 0.00721m^3/s$.

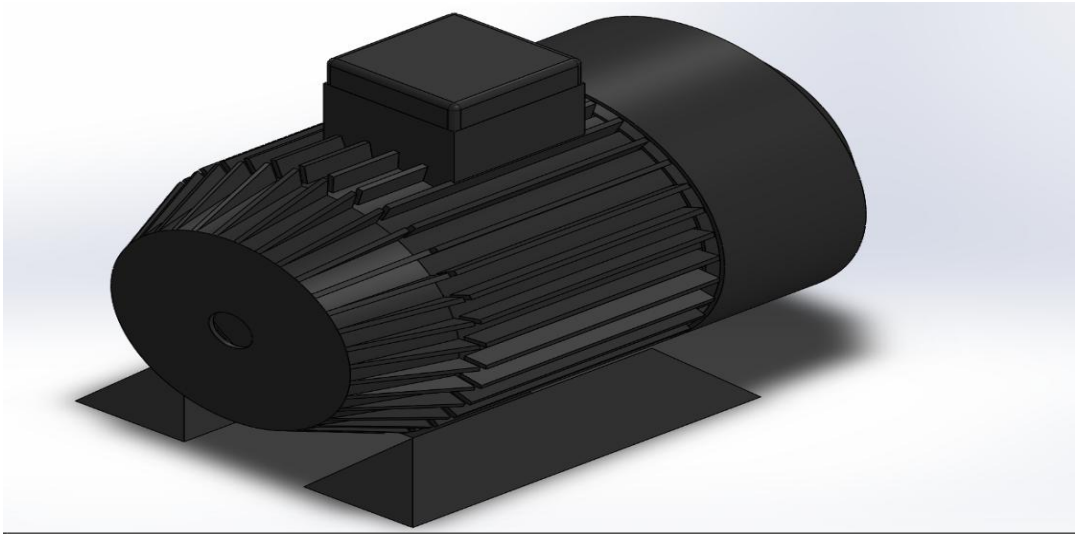


Figure 5: Shows the design of an Electric motor for the pump on solid works

2.2.5 Design of heaters

From Stefan's law; the heat quantity received by the target material from the source point, is influenced by the temperature difference between the two bodies, and the transmitting medium. The heat source is the heating element powered by electricity and the target object is substance (water).

$Stefan's\ Constant = 5.72 \text{ x } 10^4\ K\varepsilon[(\frac{T_1}{1000})^4\text{-}(\frac{T_2}{1000})^4]$ 26

Where: T_1 = temperature of heating element; T_2 = temperature of substance to be heated; K = constant; and ε = emissivity.

From heater ratings; $T_1 = 120$ ℃, $K = 0.5$, $T_2 = 20$ ℃, and $\varepsilon = 0.95$

Amount of heat generated by the heater = $0.000563w/m^2$.

For circular coil (wire);

$R = \frac{\rho l}{a} = \frac{4\rho l}{\pi d^2}$ 27

$p = \frac{v^2}{R} = \frac{\pi d^2 v^2}{4\rho l}$ 28

Where: V = voltage supply (v); R = resistance (Ω); a = area of coil = $\frac{\pi d^2}{4}$ (m^2); l = length of coil; d = diameter of coil; andρ = specific resistance.

Heater ratings: number of heating coils = 5; diameter of coil = 400mm; coupling distance = 10mm; length of coil = 15mm; coil thickness = 1.5mm; time of heat discharge = 25mins (1500s).

Power rating (220volts, 30Ω)

Heat generated per second;

$P = VI$ 29a

Where $V = IR$

$$p = \frac{v^2}{R}$$ 29b

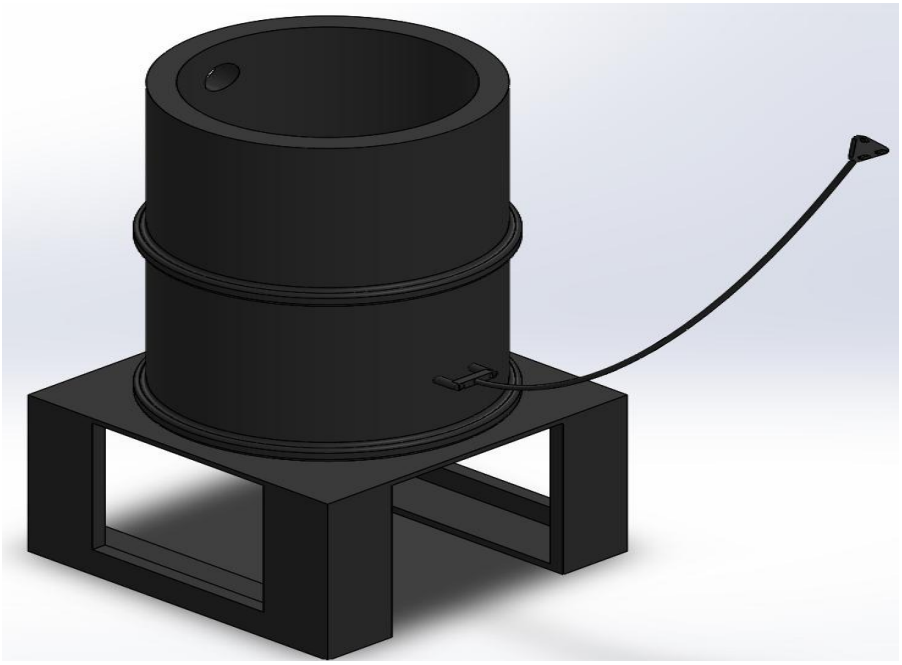


Figure 6: Design of heaters made on solid works

3.0 Results and Discussion

3.1 Design calculations

The results (values) of the design calculations of the STHE are presented in Tables 1 to 3.

Table 1: Summary of theSTHE

S/N	Description	Value	Unit
1	Shell Outer diameter	12.7	Mm
2	Shell inner diameter	12.7	Mm
3	Length of shell (Allowance for tube sheet not included)	80.0	Mm
4	Tube Outside diameter	12.75	Mm
5	Tube Inside diameter	9.5	Mm
6	Baffle Spacing (baffle cut at 25%)	15.0	Mm
7	Tube Pitch	15.875	Mm
8	Number of tubes	7.0	
9	Thermal Conductivity of tubes	677.03	W/m-k
10	Tube side**	0.0000113	W/m-k
11	Shell side**	0.000221	W/m-k
12	Clean overall**	114.7	W/m-k
13	Fouled overall**	0.00001	W/m-k
14	Number of passes	2.0	
15	Shell side pressure drop	0.40	Kpa

** = heat transfer coefficient

Table 2: Summary of the Tube Side and Shell side

TUBE SIDE:	**HOT SIDE**		
S/N	**Description**	**Value**	**Unit**
1	Inlet temperature	99.90	℃
2	Mass flow rate	7.21	Kg/s
3	Density	1000	Kg/m^3
4	Thermal conductivity	677.03	w/m-k
5	Dynamic viscosity	0.2818	$N.s/m^2$
6	Specific Heat	2.080	J/kg-k
7	Reynolds number	2.5×10^{-5}	
8	Velocity of fluid inside the tubes	0.06	mm/s
9	Total fouling factor	0.0001	M^2-k/w
SHELL SIDE:	**COLD SIDE**		
1	Inlet temperature	20	℃
2	Outlet temperature	55	℃
3	Average temperature	41.0	℃
4	Mass flow rate	7.21	Kg/s
5	Density	1000	Kg/m3
6	Thermal Conductivity	645.755	W/m - K
7	Dynamic viscosity	1.0016	$N.s/m^2$
8	Specific heat	4.184	kJ/kg - k
9	Reynolds number	800	

Table 3:Equipment and their ratings

S/N	**Equipment**	**Ratings**
1	Centrifugal pump	0.5hp
2	Heaters	220V, 30Ω
3	Reservoir	6 Liters

The materials for the STHE were specified based on the project's aim and objectives, which are to produce a STHE for distilled water production for small pharmaceutical industries using locally available materials. The design specifications, as well as the materials used, are consistent and reliable. Theshell and tube heat exchangeruncovered area, wasevaluated by the number of thermally conductive metal tubes used. Fluid flow inside a STHE can be either parallel or cross flow. The steam that flows from the tubes is expanded and condensed at the end of the shell, where distilled water is returned to the tank. Figure 4.3 depicts both the inlet and outlet nozzles on the front header of the channel side. These findings highlighted that this model predominately has an even amount of tube passes. Though, there could be instances of odd number of tube passes; and in this scenario, the channel side outlet nozzle will be on the read header, as the *h* value tends to incline as the amount of the tube passes increases. Turbulators and baffles are appropriately installed inside tubes and shells, to facilitate the fluid turbulence; thereby, enhancing the heat transfer volume between the fluids.

3.2 Assembled design of shell and tube heat exchanger

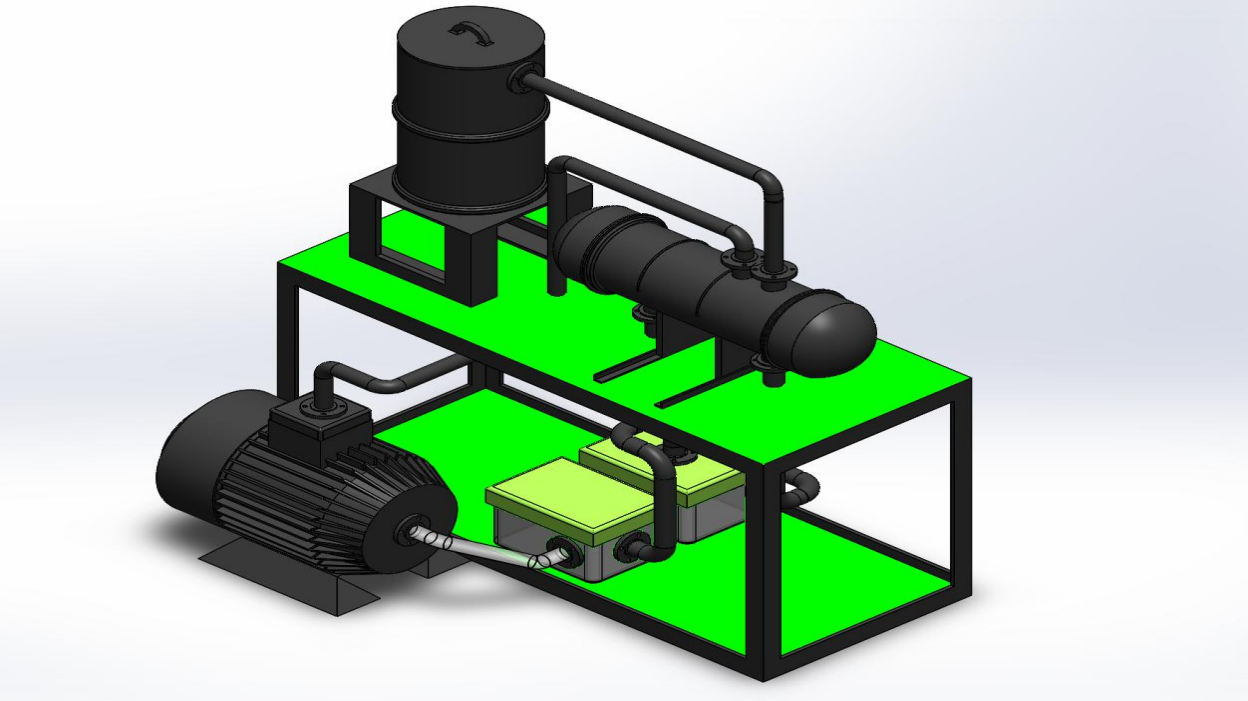


Figure 7: A design of shell and tube heat exchangers made on solid works

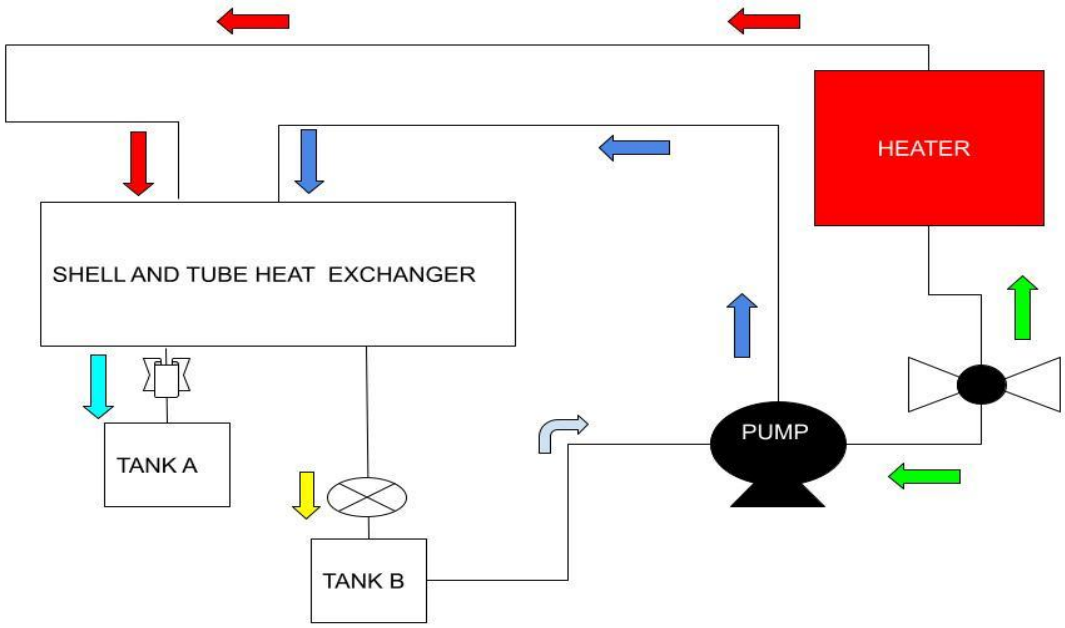


Figure 8: Schematics of the STHE.

The STHE prototype works by allowing fluid to flow inside the tubes and out through the shell. This results in adequate heat exchange, while the fluid flows through the system, leading to the cold fluid absorbing heat from the hot medium. Hence, as the cold fluid enters the system (tube side or channel side) inlet pipe and exits as a hot fluid; obviously, creating a cycling unit - another fluid becomes loss heat in the outlet. Cooling occurs when fluids mix between the shell and tube sides, and the hot steam is converted into distilled water. In addition, as the cycle continues, the cold fluid absorbs a certain amount of heat; this principle can be traced back to the first law of thermodynamics.The heaters, located next to the

reservoirs, heat the water to approximately 100 ℃. The control panel box, located next to the heat exchanger, provides power to both the pump and heater. The STHE is designed to be airtight and capable of handling high temperatures. It was discovered that temperatures on the high and low temperatures sides, are interdependent for heat to be exchanged. At first, the temperatures were far apart, but once they mixed indirectly, heat from the tube side was transferred to the SS as it flowed across, and the process became reversible.In summary, as the cold side's temperature drops, the hot side's by absorbing heat from the flow path. Furthermore, the number of tubes influences the volume and flow rate. The number of tubes increased as the volume flow rate reduces. This is an important aspect in the production of the STHE, because for cooling to be effective, it must have a reasonable length. However, because efficiency is required, optimisation comes into play, and at this point, the number of tubes in terms of length and performance against time were graded.

4.0 Conclusion

At the end of this experiment, several things must be achieved and thus concluded in order to obtain the desired result in this test, which are as follows:

1. The temperature sensor measures and detects the fluid's (water) temperature (Tc) before heating it thoroughly for the next step.
2. A heating element heats the fluid until it becomes pure vapour or steam. The temperature (Th) is then detected by a temperature sensor.
3. Steam is moved using an electric motor connected to a fan.
4. Cool air blown into the coiled tubes reduces temperature and condenses steam into distilled water.

References

Bhattacharyya, S., Vishwakarma, D. K., Srinivasan, A., Soni, M. K., Goel, V., Sharifpur, M., Ahmadi, M. H., Issakhov, A., & Meyer, J. (2022). Thermal performance enhancement in heat exchangers using active and passive techniques: A detailed review. *Journal of Thermal Analysis and Calorimetry*, *147*(17), 9229–9281. https://doi.org/10.1007/s10973-021-11168-5

Chen, L.-Y., Adi, V. S. K., & Laxmidewi, R. (2022). Shell and tube heat exchanger flexible design strategy for process operability. *Case Studies in Thermal Engineering*, *37*, 102163. https://doi.org/10.1016/j.csite.2022.102163

Estupiñán-Campos, J., Quitiaquez, W., Nieto-Londoño, C., & Quitiaquez, P. (2024). Numerical simulation of the heat transfer inside a shell and tube heat exchanger considering different variations in the geometric parameters of the design. *Energies*, *17*(3), 691. https://doi.org/10.3390/en17030691

Fernandes, D. V. (2023). Heat transfer enhancement in a tube heat exchanger using discrete triangular-prism roughness elements. *RAiSE-2023*, 62. https://doi.org/10.3390/engproc2023059062

Ghasem, N. (2021). Shell and tube heat exchangers. In *Computer Methods in Chemical Engineering* (pp. 123–207). CRC Press. https://doi.org/10.1201/9781003167365-4

Gonçalves, C. de O., Costa, A. L. H., & Bagajewicz, M. J. (2016). Shell and tube heat exchanger design using mixed-integer linear programming. *AIChE Journal*, *63*(6), 1907–1922.

Hamza, N. Fouad. A., & Aljabair, S. (2022). Evaluation of thermal performance factor by hybrid nanofluid and twisted tape inserts in heat exchanger. *Heliyon*, *8*(12), e11950. https://doi.org/10.1016/j.heliyon.2022.e11950

Han, L., Zhang, S., & Yan, Y. (2025). *Heat transfer enhancement and thermal energy storage in heat exchangers using novel bionic honeycomb core and multi-objective optimizations*. Elsevier BV. https://doi.org/10.2139/ssrn.5148295

Jayranaiwachira, N., Promvonge, P., Thianpong, C., Promthaisong, P., & Skullong, S. (2023). Effect of louvered curved-baffles on thermohydraulic performance in heat exchanger tube. *Case Studies in Thermal Engineering*, *42*, 102717. https://doi.org/10.1016/j.csite.2023.102717

Lee, J., &Leyffer, S. (2011). *Mixed integer nonlinear programming*. Springer Science & Business Media.

Math, Praveen. (2021). *Performance analysis and design optimization of shell and tube heat exchangers*. Research Square Platform LLC. https://doi.org/10.21203/rs.3.rs-407371/v1

MilaniShirvan, K., Mamourian, M., & AbolfazliEsfahani, J. (2018). Experimental investigation on thermal performance and economic analysis of cosine wave tube structure in a shell and tube heat exchanger. *Energy Conversion and Management*, *175*, 86–98. https://doi.org/10.1016/j.enconman.2018.08.103

Mohammadi, M. H., Abbasi, H. R., Yavarinasab, A., & Pourrahmani, H. (2020). Thermal optimization of shell and tube heat exchanger using porous baffles. *Applied Thermal Engineering*, *170*, 115005. https://doi.org/10.1016/j.applthermaleng.2020.115005

Mukhlif, E., & Abed, W. (2024). Procedures of exploitation passive techniques to boost thermal performance in circular tube heat exchangers: A comprehensive review. *Anbar Journal of Engineering Sciences*, *15*(2), 62–81. https://doi.org/10.37649/aengs.2024.152719.1096

Ponce-Ortega, J. M., Serna-González, M., & Jiménez-Gutiérrez, A. (2009). Use of genetic algorithms for the optimal design of shell-and-tube heat exchangers. *Applied Thermal Engineering*, *29*(2–3), 203–209. https://doi.org/10.1016/j.applthermaleng.2007.06.040

Rahman, M. A. (2024). Comprehensive Strategies for Addressing Tube and Tubesheet Joint Leaks in Shell-and-Tube Heat Exchangers. *Heat Transfer Engineering*, 1–19. https://doi.org/10.1080/01457632.2024.2427313

Rao, R. V., &Saroj, A. (2017). Constrained economic optimization of shell-and-tube heat exchangers using elitist-Jaya algorithm. *Energy*, *128*, 785–800. https://doi.org/10.1016/j.energy.2017.04.059

Tandiroglu, A. (2007). Effect of flow geometry parameters on transient entropy generation for turbulent flow in circular tube with baffle inserts. *Energy Conversion and Management*, *48*(3), 898–906. https://doi.org/10.1016/j.enconman.2006.08.022

Yang, Z., Ma, Y., Zhang, N., & Smith, R. (2020). Design optimization of shell and tube heat exchangers sizing with heat transfer enhancement. *Computers & Chemical Engineering*, *137*, 106821. https://doi.org/10.1016/j.compchemeng.2020.10682